BMC Oral Health

RESEARCH

Open Access

Fiber sleeve impact on push-out bond strength of adjustable post system

Eren Var[1], Cihan Küden[1*] and Oguz Yoldas[1]

Abstract

Purpose This study investigated the influence of the fiber sleeve on push-out bond strength (PBS), both with and without aging in a mastication simulator.

Materials and methods Sixty straight-rooted mandibular premolars were randomly divided into four groups ($n=15$). Groups S and S_{MS} included fiber sleeves and posts, while Groups P and P_{MS} included posts only. Groups S_{MS} and P_{MS} underwent aging in a mastication simulator (50 N load, 240,000 cycles). Specimens were sectioned into 1 mm slices (coronal, middle, apical thirds), and PBS testing was performed using a universal testing machine. Failure modes were analyzed under 40× magnification. Statistical analysis used one-way ANOVA and Tukey tests ($\alpha=0.05$).

Results Group S had the highest PBS, significantly surpassing Group P ($P<0.001$). Aging significantly reduced PBS in sleeve groups (S vs. $S_{MS,}$ $P=0.029$) Adhesive failure between dentin and cement was most common.

Conclusion The use of fiber sleeves significantly improved PBS; however, this enhancement diminished following aging procedures.

Keywords Adjustable post, Bond strength, Fiber post, Mastication simulator, Sleeve

Introduction

Post systems are essential for restoring extensively damaged, endodontically treated teeth, with ongoing advancements in materials and techniques improving clinical outcomes [1]. Common materials include metal alloys, ceramics, glass fiber, and carbon fiber, each with unique advantages in strength, esthetics, and adhesive compatibility [2]. Among these, glass fiber posts are most preferred due to their dentin-like elastic modulus, strong resin bonding, excellent esthetics, biocompatibility, and effective stress distribution, which minimizes the risk of root fractures and structural failures [3, 4].

The retention of glass fiber posts within the root canal is influenced by factors such as post length, diameter, surface design (e.g., smooth, serrated, or tapered), and the type of cementation material and technique [5, 6]. Notably, the thickness of the resin cement layer plays a critical role, as thicker layers can compromise push-out bond strength (PBS) due to increased polymerization shrinkage and void formation [7, 8]. To address these challenges, approaches like anatomically shaped posts or multifilament systems have been proposed to minimize resin thickness and reduce the C-factor, improving adaptation to root canal morphology [9–13].

Recently, a novel single adjustable post (SAP; Splendor, Angelus, Londrina, PR, Brazil) system has been developed, comprising a universal cylindrical post and a conical fiber sleeve that adapts to the root canal without requiring additional preparation. This system promotes uniform distribution of a thinner resin cement layer,

*Correspondence:
Cihan Küden
ckuden@cu.edu.tr
[1]Department of Endodontics, Faculty of Dentistry, Cukurova University, Adana 01380, Turkey

© The Author(s) 2025. **Open Access** This article is licensed under a Creative Commons Attribution-NonCommercial-NoDerivatives 4.0 International License, which permits any non-commercial use, sharing, distribution and reproduction in any medium or format, as long as you give appropriate credit to the original author(s) and the source, provide a link to the Creative Commons licence, and indicate if you modified the licensed material. You do not have permission under this licence to share adapted material derived from this article or parts of it. The images or other third party material in this article are included in the article's Creative Commons licence, unless indicated otherwise in a credit line to the material. If material is not included in the article's Creative Commons licence and your intended use is not permitted by statutory regulation or exceeds the permitted use, you will need to obtain permission directly from the copyright holder. To view a copy of this licence, visit http://creativecommons.org/licenses/by-nc-nd/4.0/.

potentially enhancing dentin bonding and biomechanical performance [10, 11, 14–16]. Studies have indicated that SAP systems outperform conventional and anatomical posts in terms of PBS and stress distribution under fatigue conditions [10, 17–20]. However, there is limited evidence on the long-term adhesive interface performance of SAP systems in oval or severely damaged root canals.

It is essential to test and analyze restorations under conditions that closely simulate the oral environment to ensure their clinical reliability [21–24]. Among in vitro methods, mastication simulators are particularly effective for this purpose. These devices replicate functional stresses through cyclic loading over extended periods, simulating clinical conditions and enabling a detailed evaluation of the adhesive properties and durability of post systems. Assessing the effects of mastication-induced aging provides critical insights into the long-term performance and reliability of post-core restorations.

A comprehensive review of the literature reveals a lack of studies evaluating the effectiveness of the fiber sleeve within the SAP system. To address this gap, the present study investigates the impact of the fiber sleeve on the bond strength and biomechanical performance of endodontically treated teeth. By comparing groups with and without fiber sleeves, the study aims to assess the effects of reduced resin cement thickness on PBS, adhesive interface integrity, and overall system performance under mastication-induced aging. The hypotheses tested are as follows: (i) there is no significant difference in bond strength between fiber sleeve and non-sleeve groups in the absence of aging, and (ii) aging does not significantly affect the bond strength of the SAP system.

Materials and methods

Ethical approval for this study was obtained from the Cukurova University Non-Interventional Clinical Research Ethics Committee (Approval No: 2023/131/20). Mandibular teeth extracted for orthodontic or periodontal reasons were used in this study. Written and verbal informed consent was obtained from individuals for the use of their teeth in this research. The specimen size was determined based on hypothetical values using G*Power 3.1 software (Heinrich Heine University, Düsseldorf, Germany). With a power of 95%, a significance level of 0.05, and an effect size of 0.60, the minimum required specimen size per group was calculated to be 13. However, for this in vitro study, analyses were conducted using 15 specimens per group to ensure robustness.

Specimen Preparation

To ensure disinfection and structural preservation, sixty recently extracted, caries-free single-rooted mandibular premolars were cleaned and stored at 37 °C in a 0.5% thymol solution. Specimens were examined under 10× magnification to exclude those with cracks or fractures, and periapical radiographs in buccolingual and mesiodistal orientations were used to confirm the presence of an open and continuous root canal system, as well as to rule out canal resorption and previous endodontic treatment. Coronal segments were sectioned perpendicular to the tooth's long axis, 2.0 mm above the cementoenamel junction, to maintain adequate coronal structure and achieve a ferrule effect. All specimens were standardized to a total length of 17.5 mm (15.5 mm root + 2.0 mm coronal structure).

Root Canal Preparation

A #10 K-file was used to create a glide path and confirm canal patency. The file was gently advanced until its tip became visible at the apical foramen, after which the working length was determined by subtracting 1 mm from this measurement to preserve apical anatomy and ensure standardization across specimens. Canal instrumentation was performed using R25, R40, and R50 files with an electronic endomotor (VDW Gold Reciproc motor, VDW, Munich, Germany) following the crown-down technique. The shaping protocol was applied conservatively, with respect to the original canal anatomy, to avoid unnecessary removal of dentin. All specimens were irrigated using a standardized protocol after each instrumentation step. A fresh solution was used for each specimen, and the irrigants were delivered passively up to 1 mm short of the working length using a conventional irrigation needle. After each file, canals were irrigated with 2 ml of 2.5% NaOCl, followed by final irrigation with 2 ml of 5% EDTA and 10 ml of distilled water. The canals were dried with paper points (Dentsply Tulsa Dental, OK, USA). The size #50 gutta-percha master cones were selected to match the final apical size (R50), and tug-back was confirmed prior to sealer application. Obturation was completed using the cold lateral compaction technique. A size #50 gutta-percha master cone was coated with AH Plus sealer (Dentsply DeTrey, Konstanz Germany) and inserted to full working length. Finger spreaders were used to place accessory gutta-percha cones with light apical pressure, advancing until slight resistance was encountered, to avoid overcompaction and ensure homogeneous lateral filling. Root canal orifices were sealed with temporary filling material (Cavit-G; 3 M ESPE, Germany) and stored at 37 °C in 95% humidity for 7 days. All root canal shaping and obturation procedures were performed by a single experienced operator (E.V.) to ensure standardization across specimens.

Post space prepration

After one week, the temporary fillings were removed. Gutta-percha was extracted using #3 and #4 Gates-Glidden drills to a depth of 13.5 mm, preserving a 4 mm apical seal. The root canals were irrigated with 5 ml of 17% EDTA followed by 5 ml of physiological saline to eliminate residual obturation material, and then dried with paper points. For post space preparation, Gates-Glidden drills (#6–5–4) were used in a stepwise manner to create a tapered post space, ensuring dimensional consistency among specimens. This was followed by the use of the dedicated drill provided in the Splendor-SAP system (Splendor SAP; Angelus, PR, Brazil). Care was taken to ensure that the fiber sleeve was seated to a depth of 9 mm in both the sleeve and no-sleeve groups. The fiber sleeve's elliptical-like cross-sectional geometry and semi-flexible structure allowed it to adapt to the prepared canal space under light pressure.

Post cementation

All Posts were disinfected with alcohol, dried with air spray, and treated with a silane coupling agent (G-Multi Primer, GC Tokyo, Japan) for 60 s before air drying. Teeth were randomly assigned into four groups (Fig. 1). *Group S*: Both post and sleeve components of the SAP system were used without core build-up, and teeth were not subjected to mastication simulation. *Group* S_{MS}: Post and sleeve components were cemented, followed by composite resin core build-up, metal crown placement, and aging in a mastication simulator. *Group P*: Only the post component was used without the sleeve or core build-up, and teeth were not subjected to mastication simulation. *Group* P_{MS}: Only the post component was cemented without the sleeve, followed by composite resin core build-up, metal crown placement, and aging in a mastication simulator.

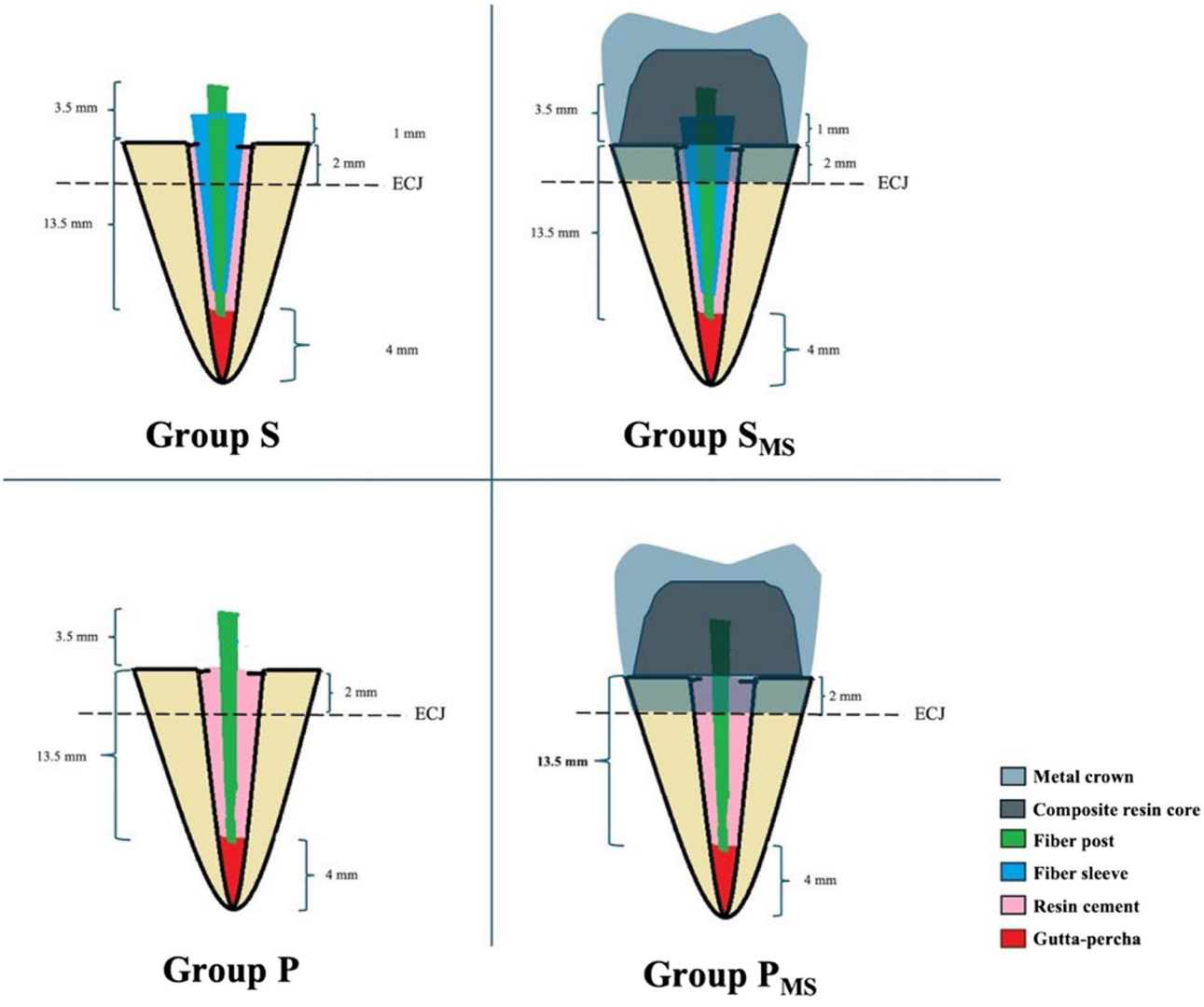


Fig. 1 Represantative preparation of the experimantel groups

In all groups, Panavia SA Cement (Kuraray, Okayama, Japan) was applied to the canals using an intracanal tip, and posts were placed within 40 s. Light curing was performed for 20 s with a LED device (Elipar S10; 3 M ESPE, USA), followed by 5 min of chemical curing. Specimens were stored at 37 °C with 95% humidity for 48 h. To ensure uniform cement adaptation, a tapered post space preparation protocol was applied using Gates-Glidden drills followed by the system-specific Splendor-SAP drill. This allowed for consistent internal canal shaping and reduced variation in the spatial relationship between the post, dentin, and fiber sleeve. All procedures including post space preparation and post cementation were carried out by a single endodontist (E.V.) with extensive clinical experience, minimizing operator variability and ensuring procedural consistency.

Crown Fabrication, mastication Simulation, and thermal cycling

In the S_{MS} and P_{MS} groups, teeth were air-dried, universal adhesive (GC Solare Universal Bond, GC, Tokyo, Japan) was applied, air-thinned for 10 s, and light-cured for 10 s. A seven mm composite core (GC Dental Genial Posterior Composite, Japan) was shaped using a water-cooled high-speed handpiece (KaVo, Germany) with diamond burs, creating round-shoulder designs terminating at the cemento-enamel junction and standardized to 5 mm.

Specimens from the S_{MS} and P_{MS} groups were embedded in 30 mm wax blocks (five per block). Digital impressions were obtained with an intraoral scanner (3Shape Trios A/S, Copenhagen, Denmark) and sent for 2 mm metal crown fabrication via laser sintering. Crowns were checked for fit and cemented with polycarboxylate cement (Adhesor Carbofine, Pentron, Czech Republic).

To simulate the periodontal membrane, roots were coated with a 0.2–0.3 mm wax layer using the melted wax immersion method, embedded in 30 mm PVC blocks with self-cured acrylic resin, and removed after the acrylic partially hardened. The wax was cleaned, and low-viscosity polyvinyl siloxane (Elite HD+, Zhermack, Italy) was injected into the spaces to form an artificial periodontal membrane. Crowned specimens were replaced into the acrylic blocks and aged in a chewing simulator (MOD, Esetron Smart Robotechnologies, Ankara, Turkey) under a vertical speed of 60 mm/s, vertical movement of 5 mm, horizontal speed of 60 mm/s, horizontal movement of 1 mm, and a 50 N force for 240,000 cycles at 1.67 Hz. Thermal cycling between 5 °C and 55 °C was applied during the simulation.

Sectioning and push-out bond strength testing

Specimens were mounted in transparent acrylic blocks for precision cutting (Struers Accutom 10, OH, USA). Fiber-post cemented roots were trimmed at the enamel-cement junction using a water-cooled diamond saw. A total of 180 dentin discs (1 ± 0.05 mm thick) were obtained from the coronal, middle, and apical regions of all groups, with 2 mm spacing between sections, as shown in Fig. 2.

The push-out test was performed using a universal testing machine (Testometric M500, 25 kN; Rochdale, UK) with a crosshead speed of 0.5 mm/min. A 1 mm diameter push pin was aligned to the center of the post surface.

The bonding surface area of each section was calculated using the lateral surface area formula of a truncated cone:

$$A = \pi \left(R_1 + R_2 \right) \sqrt{\left[\left(R_1 - R_2 \right)^2 + h^2 \right]}$$

where π is approximately 3.1416, R_1 and R_2 are the coronal and apical radii (in mm), respectively, and h is the slice thickness (1 mm). The coronal and apical diameters of each specimen were measured individually using a stereomicroscope under 40× magnification and a digital caliper (accuracy: 0.01 mm).

This formula is commonly used in PBS studies and was adopted based on previously published methods [15, 25]. PBS value was calculated in megapascals (MPa) by dividing the maximum failure load (Newton) by the bonded surface area (mm^2).

Failure mode analysis

Failure modes were classified based on failure modes by consensus between two calibrated operators using a operation microscopy (iSee 9000; Woodpecker Medical Instrument Co., Guilin, China) at 40× magnification. The sections were categorized into four modes of failure: Adhesive failure between the dentin and resin cement, adhesive failure between the post and resin cement, mixed failure (partial coverage of the post section by resin cement), and cohesive failure within the fiber post.

Statistical analysis

All analyses were performed using SPSS Statistics version 29.0.1.1 for MAC (IBM, Armonk, NY, USA) program. The homogeneity of the obtained data was analyzed using the Shapiro-Wilk test. Statistical differences between the bond strengths of the groups were evaluated using one-way ANOVA and Tukey post-hoc tests.

To compare failure mode distributions across coronal, middle, and apical thirds, chi-square tests were performed separately for each level. For statistical validity, the 'post–cement adhesive' category was excluded from the analysis due to its very low and uneven frequency across groups, which would compromise the reliability of the test. When overall significance was detected, pairwise comparisons were performed with Bonferroni correction to control for multiple testing.

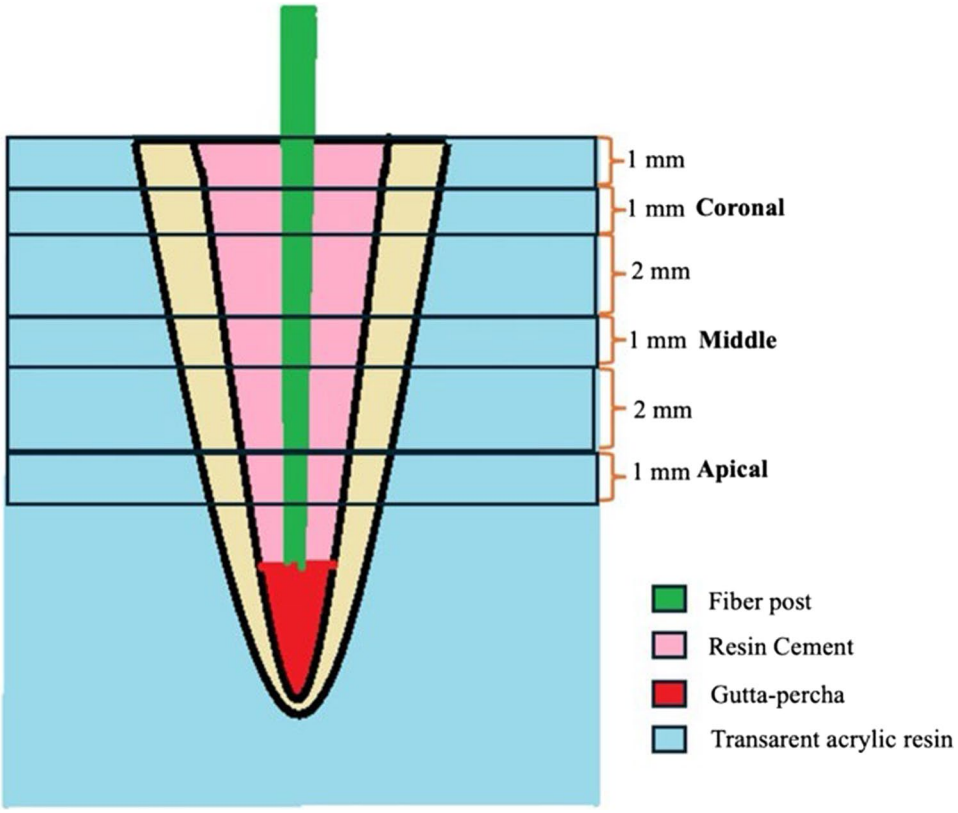


Fig. 2 Representative sectioning of the specimen

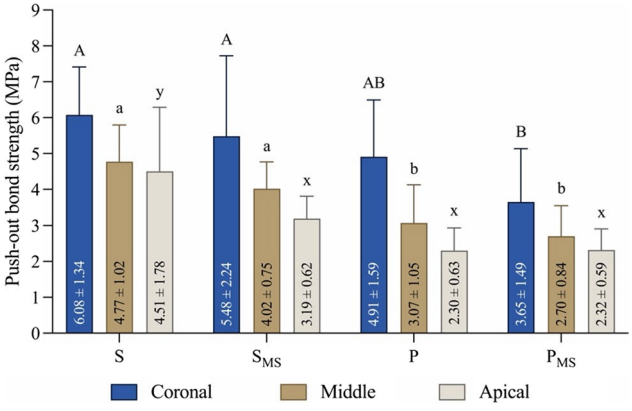


Fig. 3 The mean and standard deviation values for push-out bond strength (PBS) and the corresponding statistical analysis results were calculated for the coronal, middle, and apical root regions in each group. Capital letters (**A, B**) indicate significant statistical differences in PBS at the coronal third, lowercase letters (**a**, **b**) denote differences at the middle third, and lowercase letters (x, y) represent differences at the apical level

For overall comparisons of failure modes in pooled data across all root levels, a Fisher's Exact Test with Monte Carlo simulation (10,000 samples) was used to accommodate small cell sizes. However, pairwise comparisons among groups were not conducted in this pooled dataset due to the presence of multiple zero-frequency cells, which violated the assumptions required for reliable Fisher's tests and rendered post-hoc subgroup analyses statistically unstable. ($\alpha = 0.05$).

Results

Push-out bond strength

The mean PBS values and their standard deviations, along with the statistical comparisons across the three root regions—coronal, middle, and apical thirds—are presented in Fig. 3. At the coronal, middle, and apical levels, one-way ANOVA revealed statistically significant differences among the groups ($F(3, 59) = 5.559$, $P = 0.002$; $F(3, 59) = 15.348$, $P < 0.001$; and $F(3, 59) = 18.710$, $P < 0.001$, respectively).

At the coronal level, the S group exhibited the highest PBS value. While there was no significant difference between the S and P groups at the coronal level ($P = 0.247$), the S group demonstrated significantly higher PBS values compared to the P group at the middle and apical levels ($P < 0.001$ for both). The S group showed similar PBS values to the S_{MS} group at the coronal and middle levels ($P = 0.773$ and $P = 0.128$, respectively); however, at the apical level, the S group exhibited significantly higher PBS values than the S_{MS} group ($P = 0.005$). No significant differences were observed between the P and P_{MS} groups across all three root regions ($P = 0.192$, $P = 0.691$, and $P = 0.999$, respectively).

Among the aged groups subjected to the mastication simulator, the PBS values in the P_{MS} group were significantly lower than those in the S_{MS} group at both the coronal and middle regions ($P = 0.023$ and $P = 0.001$, respectively). Within all groups, comparisons across root sections revealed that the coronal region consistently exhibited significantly higher PBS values than the middle and apical regions ($P < 0.05$).

The mean PBS values, standard deviations, and statistical comparisons for each group are presented in Fig. 4. When the overall PBS values across all sections were compared, the S group displayed the highest values, significantly differing from the S_{MS}, P, and P_{MS} groups ($P = 0.029$, $P < 0.001$, and $P < 0.001$, respectively).

Failure modes

A chi-square test was performed to compare the distribution of failure modes (adhesive at dentin–cement or post–cement interface, cohesive, and mixed) among experimental groups at the apical, middle, and coronal levels. The overall chi-square analysis revealed a statistically significant difference in failure mode distribution among the groups at both the apical ($P = 0.038$) and coronal ($P = 0.041$) levels. However, subsequent pairwise comparisons with Bonferroni correction did not reveal any statistically significant differences between individual group pairs (adjusted $P > 0.05$ for all comparisons). Therefore, although the overall chi-square test indicated heterogeneity in failure patterns, no specific group comparison reached statistical significance when corrected for multiple testing.

Adhesive failures at the dentin-cement interface, adhesive failures at the post-cement interface, mixed failures, and cohesive failures were all observed in this study. Representative images of the four failure modes are presented in Fig. 5. The percentage distribution of failure modes in the root regions for each group is illustrated in Fig. 6. Adhesive failures at the dentin-cement interface and mixed failures were observed across all groups. Adhesive failures at the post-cement interface were noted only in specific regions: 7% in the coronal region of the S_{MS} group, 13% in the middle region of the P group, and 7% in the middle region of the P_{MS} group. Cohesive failures were exclusively observed in the S and S_{MS} groups.

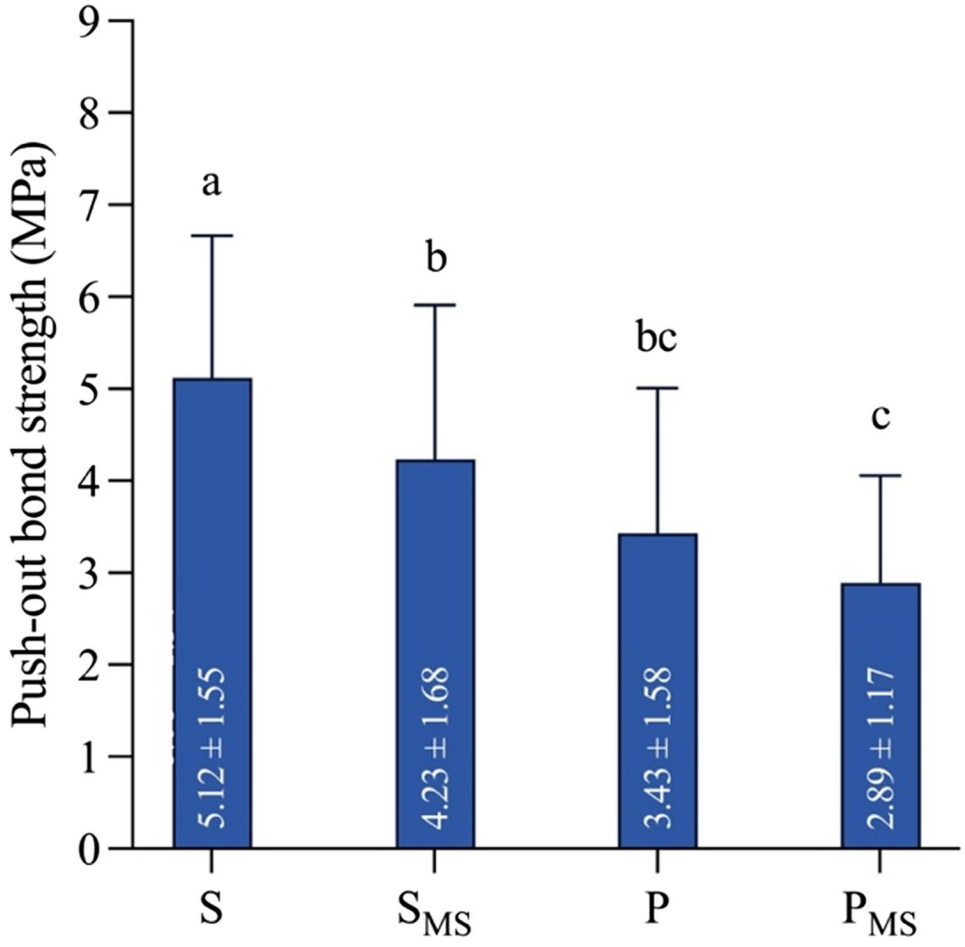


Fig. 4 Mean and standard deviation values of the total push-out bond strength for each group, along with statistical comparisons

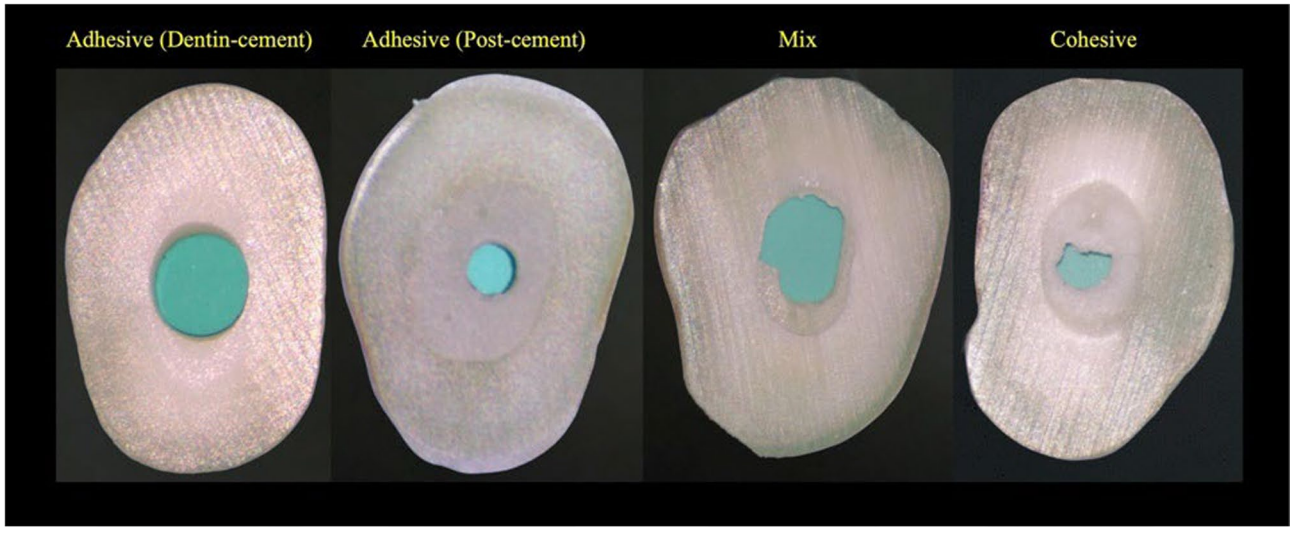


Fig. 5 Representative images of the failure modes

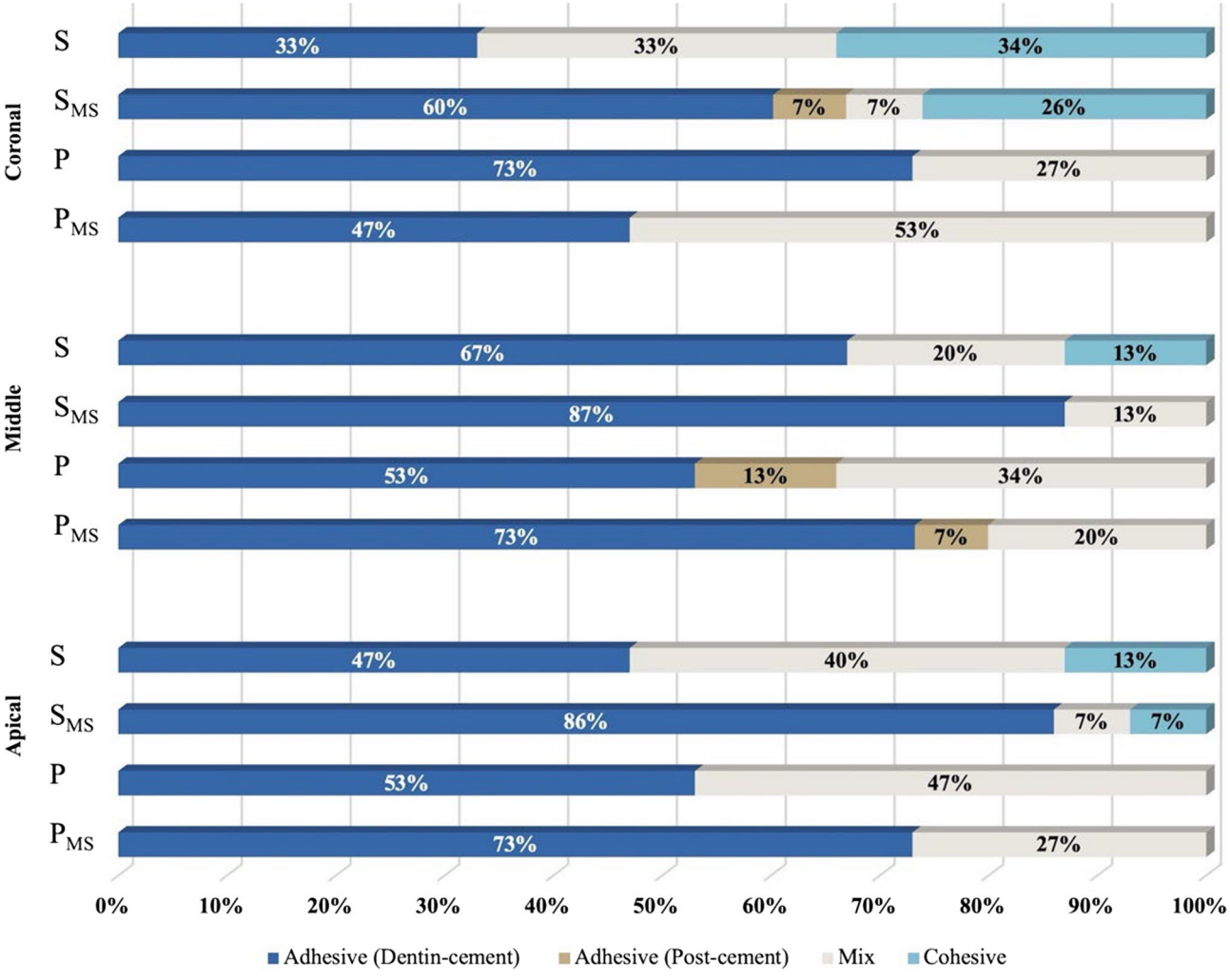


Fig. 6 Percentage distribution of failure modes across root regions for each group

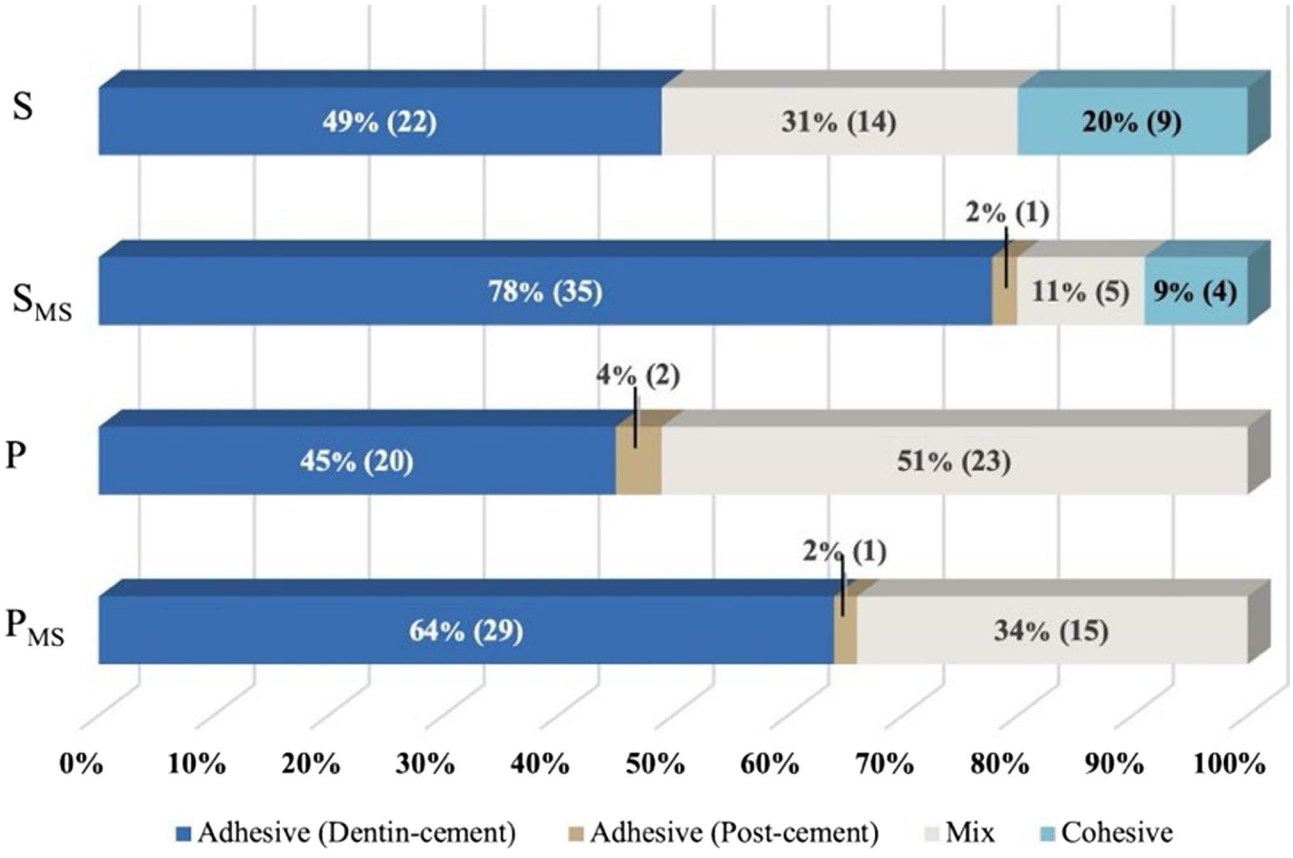


Fig. 7 Overall distribution of failure modes by group

The highest rate of cohesive failure (34%) was found in the coronal region of the S group, followed by the S_{MS} group at 26%. In the middle and apical regions, the S group exhibited the highest cohesive failure values. Adhesive failure at the dentin-cement interface was most prevalent in the coronal region of the P group. For the middle and apical regions, the highest percentages of adhesive failures at the dentin-cement interface were observed in the S_{MS} group (87% and 86%, respectively), followed by the P_{MS} group, which recorded 73% in both regions.

The overall rates and numbers of failure modes are summarized in Fig. 7. When examining the total distribution, specimens subjected to aging in the chewing simulator demonstrated a higher prevalence of dentin-cement interface failures in both systems with and without fiber sleeves. In aged specimens, the proportion of mixed failures decreased, shifting predominantly toward adhesive failures at the dentin-cement interface.

To evaluate differences in overall failure mode distribution across the experimental groups, Fisher's Exact Test with Monte Carlo simulation (10,000 resamples; seed = 112562564) was employed as a robust non-parametric alternative, owing to the presence of low expected cell counts in the contingency table. The test revealed a statistically significant association between failure mode and group allocation ($F(9, N = 180) = 34.516$, $P < 0.001$), demonstrating that failure patterns were not uniformly distributed across the groups. Nevertheless, the presence of multiple zero-frequency cells precluded reliable pairwise comparisons. As such, while the global analysis confirmed overall heterogeneity in failure mode distribution, intergroup comparisons should be interpreted with appropriate caution due to analytical constraints.

Discussion

This study evaluated the impact of the sleeve component of the SAP system on PBS under mastication simulator-induced aging. The sleeve component demonstrated significantly higher PBS values across different root regions. Moreover, in the group utilizing the sleeve, PBS values significantly decreased following aging in the mastication simulator. Consequently, the hypotheses of this study were rejected.

In this study, the PBS test was selected as the method for evaluating post retention due to its practicality, reproducibility, and clinical relevance in assessing the adhesive interface within root canal systems. Compared to microtensile (μTBS) and shear bond strength (SBS) tests, which are more suitable for flat and accessible surfaces,

the push-out test is better adapted to the complex internal geometry of root canals [26]. The μTBS method offers high sensitivity but requires complex specimen preparation and is associated with a higher risk of pre-test failures, particularly in anatomically tapered post spaces. Similarly, SBS testing does not adequately simulate the intraradicular environment and is less representative of clinical conditions [27]. The push-out technique allows for regional analysis (coronal, middle, apical), and provides more consistent results with simpler specimen preparation. This makes it the preferred method in many recent studies investigating post–dentin adhesion [14, 15, 28]. The segmental analysis afforded by this method also enhances our understanding of how bonding performance may vary along the root length. Given these advantages, the use of the push-out test in the present study ensured that the effects of the fiber sleeve design could be evaluated under conditions closely approximating those found in clinical scenarios, while minimizing variability due to technique sensitivity or test limitations.

Although testing human teeth presents challenges, such as individual variability in mechanical properties and anatomical differences, it is highlighted that extracted human teeth are the preferred choice for in vitro testing [29]. Artificial models cannot fully replicate natural dentin, and bond strength measurements between dentin and post may not accurately reflect clinical conditions. Furthermore, bovine teeth are less suitable for PBS testing due to their significant structural and mechanical differences from human teeth [30, 31]. In this study, caries-free and fracture-free mature human teeth were selected to better approximate clinical conditions. Specifically, single-rooted mandibular premolars with straight roots were chosen due to their anatomically wide oval root canal morphology in the buccolingual direction and their compatibility with fiber post auxiliary components, as supported by previous fiber post and push-out studies [7, 11, 12].

To simulate intraoral conditions, methods such as thermal cycling, mastication simulators, storage in solutions, mechanical fatigue testing, pH variation testing, chemical aging, and high-pressure and heat testing are utilized. These techniques are critical for reliably evaluating the long-term durability, biomechanical performance, and potential failure mechanisms of restorative materials prior to clinical application. Among these, the mastication simulator distinguishes itself by closely replicating dynamic and functional intraoral stresses through dual-axis repetitive mechanical loading combined with thermal stress, providing a realistic assessment of restoration durability and performance under simulated clinical conditions [21, 22]. Therefore, a mastication simulator was employed in this study.

To date, no studies have directly investigated the biomechanical implications of resin cement occupying the internal volume of hollow fiber sleeves such as those used in the SAP system. This lack of data highlights a current gap in the literature, which this study aims to begin addressing by evaluating the bonding performance and structural integration of such sleeve–cement–post assemblies. In the current literature, a study has been identified in which the SAP system was aged chemically using 0.4% sodium azide, resulting in a significant reduction in PBS values [15]. However, to date, no study has been found that analyzes the PBS values of the SAP system after aging in a mastication simulator. According to the literature, 240,000 cycles are reported to be equivalent to one year of clinical use [32], and this study simulated one year of aging. Aging of glass fiber-based posts in mastication simulators has yielded varying results. Farina et al. [21] performed a chewing simulation of 250,000 cycles and found no significant difference in PBS values between aged and non-aged specimens. In contrast, Cecchina et al. [22] and Köle et al. [23] reported that 250,000 cycles of mastication simulation resulted in a significant decrease in PBS values. In the present study, mastication simulator aging did not yield a significant difference in PBS values for the group where the post was used alone; however, a significant decrease was observed in the group incorporating the sleeve.

Studies have demonstrated that the push-out bond strength of glass fiber posts significantly decreases with the use of thicker resin cement layers [7, 8]. This phenomenon is attributed to the C-factor, which amplifies polymerization shrinkage and results in voids within the resin cement layer [33, 34]. Therefore, optimizing resin cement thickness by considering root canal anatomy is essential when selecting glass fiber posts [5, 8, 35]. To address this issue, the newly developed SAP system has been introduced, though studies on its bond strength to root canals remain limited. Alves Dos Santos et al. [15] compared the SAP system to conventional fiber posts and reported that, among non-aged specimens, the SAP system exhibited significantly higher bond strength. After six months of chemical aging, both systems showed reduced bond strength, but the SAP system maintained significantly higher values across all root regions. Similarly, Lopes et al. [14] compared the PBS values of SAP and custom-fitted fiber posts adapted with resin. Despite no significant differences in PBS between resin types or root regions, the SAP system achieved notably higher PBS values compared to conventional posts. In our study, groups using the complete SAP system (fiber sleeve + post) demonstrated significantly higher PBS values than those using the post alone. The SAP system achieved improved post adaptation by providing homogeneous integration between the post, sleeve, and cement. Moreover, the

fiber sleeve of the SAP system acted as an auxiliary post, enhancing bond strength in expanded and compromised root canals [16]. In contrast, the lower bond strength observed in the post-only group can be attributed to shrinkage stresses caused by the thicker cementation layer [36]. Regardless of post type or aging, the highest bond strength was observed in the coronal region. This can be attributed to enhanced polymerization in the coronal region due to more effective light activation and the increased penetration of resin cement into the larger dentinal tubules present in this area [25, 37].

Lopes et al. [14], in their investigation of failure modes for SAP and customized post systems, reported that cohesive failure was observed exclusively in the SAP groups. Similarly, Alves Dos Santos et al. [15], in their study comparing SAP with conventional fiber posts, found a higher incidence of cohesive failure in the SAP system compared to conventional fiber posts. Both studies identified adhesive failure at the dentin-cement interface as the most prevalent failure mode, consistent with the findings of our study. Additionally, Alves Dos Santos et al. [15] compared the failure modes of SAP and conventional fiber posts before and after six months of aging. In alignment with our findings, their study revealed an increased rate of adhesive failure at the dentin-cement interface in aged groups.

This study has several limitations that should be acknowledged. Although efforts were made to standardize the post space geometry through stepwise canal enlargement using Gates-Glidden drills followed by refinement with the dedicated SAP system drill, natural anatomical variability in human teeth remains an inherent limitation of in vitro studies. The use of this instrumentation protocol was based on the need to achieve consistent internal canal dimensions across all specimens. Direct quantification of resin cement thickness was not performed, which may be considered a limitation. However, the use of a controlled and tapered canal preparation protocol is widely accepted in the literature as an effective indirect method to promote consistency in cement distribution and reduce bonding variability [9, 13, 33]. In the sleeve-assisted group, the resin cement occupied both the interface between the post and dentin as well as the internal lumen of the fiber sleeve. Due to its inner C-shaped cross-sectional configuration, the sleeve does not form a closed cylindrical structure. This design enables the cement to integrate within both internal and peripheral spaces, forming a unified post–sleeve–cement complex. As a result, conventional definitions of cement thickness may not fully apply to this integrated system. Finally, although a mastication simulator was used to simulate functional loading, future studies may improve upon this by incorporating longer aging durations or increased cyclic loading. Additionally, the absence of a conventional fiber post control group may be viewed as a limitation; however, this choice was intentional to isolate the specific effect of the fiber sleeve component. Future studies incorporating advanced imaging techniques such as SEM, micro-CT, or confocal laser scanning microscopy may provide further insight into the structural integrity of the sleeve–post interface following aging.

Conclusions

The SAP system groups incorporating the fiber sleeve exhibited significantly higher PBS values compared to groups without the sleeve. Although aging procedures resulted in a reduction in bond strength, this decrease was statistically significant only in certain comparisons. Notably, cohesive failures were observed exclusively in the fiber sleeve groups, underscoring the sleeve's role in enhancing the structural integrity of the SAP system.

Abbreviations

PBS	Push-out bond strength
Group S	Single adjustable post and sleeve together
Group S_{MS}	Single adjustable post and sleeve together, aged in mastication simulator
Group P	Single adjustable post only
Group P_{MS}	Single adjustable post only, aged in mastication simulator
SAP	Single adjustable post
NaOCl	Sodium hypochlorite
EDTA	Ethylenediamine tetraacetic acid
MPa	Megapascal

Acknowledgements

This research supported by Scientific Research Projects Coordination Unit of Cukurova University as specialty thesis in Endodontics (Project number: TDH-2023-15829). The authors would like to thank Cumali Yapar, CDT, for his assistance in crown production at the Prosthetic Laboratory of the Faculty of Dentistry, Cukurova University. The authors also extend their gratitude to Taha Yasin Berk, DDS, and Burçe Aktan, DDS, for their valuable support.

Authors' contributions

Author contribution Conceptualization: O.Y., E.V.; methodology: O.Y., E.V., and C.K.; Validation: C.K.; formal analysis C.K.; writing—original draft preparation: C.K., and E.V.; writing—review and editing: C.K., E.V., and O.Y.; Project administration: E.V., and O.Y.; resources: E.V., and O.Y.; supervision: C.K., E.V., and O.Y.

Data availability

The datasets used and/or analysed during the current study are available from the corresponding author on reasonable request due to privacy reasons and large data size.

Declarations

Ethics approval and consent to participate

The method performed in the present study involving human participants were in accordance with the ethical standards of the institutional and/or national research committee and with the 1964 Helsinki Declaration and its later modifications or comparable ethical standards. The present study and the protocol were found medically appropriate with the ethics committee report numbered 2023/131/20 of Cukurova University Non-Interventional Clinical Research Ethics Committee.
The written informed consent was obtained from all individual participants included in the study.

Consent for publication

Not applicable.

Competing interests
The authors declare no competing interests.

Received: 8 January 2025 / Accepted: 25 September 2025
Published online: 21 October 2025

References

1. Monticelli F, Goracci C, Ferrari M. Micromorphology of the fiber post-resin core unit: a scanning electron microscopy evaluation. Dent Mater. 2004;20(2):176–83. https://doi.org/10.1016/S0109-5641(03)00089-7.
2. Ferrari M, Vichi A, García-Godoy F. Clinical evaluation of fiber-reinforced epoxy resin posts and cast post and cores. Am J Dent. 2000;13(Spec No):b15–8.
3. Smidt A, Venezia E. Techniques for immediate core buildup of endodontically treated teeth. Quintessence Int. 2003;34(4):258–68.
4. Leong DJX, Yap AUJ. Quality of life of patients with endodontically treated teeth: a systematic review. Aust Endod J. 2020;46(1):130–9. https://doi.org/10.1111/aej.12372.
5. Soares PM, Morgan LF, Tonelli SQ, Limeira FI, Bruzinga FF, Seraidarian PI, et al. Effect of different resin cements on the bond strength of custom-made reinforced glass fiber posts-a push-out study. J Contemp Dent Pract. 2021;22(3):219–23. https://doi.org/10.5005/jp-journals-10024-3058.
6. Bertolini GR, Alves Dos Santos GN, Paula-Silva FWG, Silva-Sousa AC, Roperto R, Sousa-Neto MD, et al. Impact of the removal of filling material from the post space with ultrasonic insert and magnification with a surgical microscope on the bond strength and adhesive interface of multifilament fiberglass posts onto flat-oval root canals. J Mech Behav Biomed Mater. 2022;132:105264. https://doi.org/10.1016/j.jmbbm.2022.105264.
7. Eid RY, Koken S, Baba NZ, Ounsi H, Ferrari M, Salameh Z. Effect of fabrication technique and thermal cycling on the bond strength of CAD/CAM milled custom fit anatomical post and cores: an in vitro study. J Prosthodont. 2019;28(8):898–905. https://doi.org/10.1111/jopr.13101.
8. Chidoski-Filho JC, Camargo LP, Bittencourt BF, Reis A, Gomes OMM, Gomes JC, et al. Influence of alternative restoration technique with different composite resins for flared root reinforcement. J Adhes Dent. 2020;22(4):353–63. https://doi.org/10.3290/j.jad.a44866.
9. Freitas TL, Vitti RP, Miranda ME, Brandt WC. Effect of glass fiber post adaptation on push-out bond strength to root dentin. Braz Dent J. 2019;30(4):350–5. https://doi.org/10.1590/0103-6440201902491.
10. Penteado MM, de Andrade GS, Araujo RM, Borges ALS, Valandro LF, Pereira GKR, et al. Fatigue survival of endodontically treated teeth restored with different fiber-reinforced composite resin post strategies versus universal 2-piece fiber post system: an in vitro study. J Prosthet Dent. 2023;129(3):456–63. https://doi.org/10.1016/j.prosdent.2021.05.020.
11. Rengo C, Spagnuolo G, Ametrano G, Juloski J, Rengo S, Ferrari M. Micro-computerized tomographic analysis of premolars restored with oval and circular posts. Clin Oral Investig. 2014;18(2):571–8. https://doi.org/10.1007/s00784-013-0982-7.
12. Fernandes V, Silva AS, Carvalho O, Henriques B, Silva FS, Özcan M, et al. The resin-matrix cement layer thickness resultant from the intracanal fitting of teeth root canal posts: an integrative review. Clin Oral Investig. 2021;25(10):5595–612. https://doi.org/10.1007/s00784-021-04070-9.
13. Marcos RM, Kinder GR, Alfredo E, Quaranta T, Correr GM, Cunha LF, et al. Influence of the resin cement thickness on the push-out bond strength of glass fiber posts. Braz Dent J. 2016;27(5):592–8. https://doi.org/10.1590/0103-6440201600886.
14. Duarte Santos Lopes L, da Silva Pedrosa M, Beatriz Melo Oliveira L, Maria da Silva Costa S, Aguiar Santos Nogueira Lima L. Lucisano Botelho do Amaral F. Push-out bond strength and failure mode of single adjustable and customized glass fiber posts. Saudi Dent J. 2021;33(8):917–22. https://doi.org/10.1016/j.sdentj.2021.09.003.
15. Alves Dos Santos GN, Silva-Sousa YTC, Alonso ALL, Souza-Gabriel AE, Silva-Sousa AC, Lopes-Olhê FC, et al. Evaluation of the push-out bond strength of an adjustable fiberglass post system to an endodontically treated oval root canal. Dent Mater J. 2023;42(4):532–41. https://doi.org/10.4012/dmj.2022-248.
16. Haralur SB, Al Ahmari MA, AlQarni SA, Althobati MK. The effect of intraradicular multiple fiber and cast posts on the fracture resistance of endodontically treated teeth with wide root canals. BioMed Res Int. 2018;2018:1671498. https://doi.org/10.1155/2018/1671498.
17. Lazari PC, de Carvalho MA, Del Bel Cury AA, Magne P. Survival of extensively damaged endodontically treated incisors restored with different types of posts-and-core foundation restoration material. J Prosthet Dent. 2018;119(5):769–76. https://doi.org/10.1016/j.prosdent.2017.05.012.
18. Oliveira GR, Machry RV, Cadore-Rodrigues AC, Sarkis-Onofre R, Valandro LF, Bacchi A, et al. Fatigue properties of weakened and non-weakened roots restored with CAD-CAM milled fiber post, prefabricated fiber post, or cast metal post. Oper Dent. 2022;47(6):658–69. https://doi.org/10.2341/21-032-l.
19. da Silveira Teixeira C, Santos Felippe MC, Silva-Sousa YT, de Sousa-Neto MD. Interfacial evaluation of experimentally weakened roots restored with adhesive materials and fibre posts: an SEM analysis. J Dent. 2008;36(9):672–82. https://doi.org/10.1016/j.jdent.2008.04.020.
20. Li Q, Xu B, Wang Y, Cai Y. Effects of auxiliary fiber posts on endodontically treated teeth with flared canals. Oper Dent. 2011;36(4):380–9. https://doi.org/10.2341/10-283-l.
21. Farina AP, Chiela H, Carlini-Junior B, Mesquita MF, Miyagaki DC, Randi Ferraz CC, et al. Influence of cement type and relining procedure on push-out bond strength of fiber posts after cyclic loading. J Prosthodont. 2016;25(1):54–60. https://doi.org/10.1111/jopr.12271.
22. Cecchin D, Giacomin M, Farina AP, Bhering CL, Mesquita MF, Ferraz CC. Effect of chlorhexidine and ethanol on push-out bond strength of fiber posts under cyclic loading. J Adhes Dent. 2014;16(1):87–92. https://doi.org/10.3290/j.jad.a30556.
23. Kole S, Ergun G. Bond strength of various post-core restorations with different lengths and diameters following cycle loading. J Mech Behav Biomed Mater. 2023;142:105804. https://doi.org/10.1016/j.jmbbm.2023.105804.
24. Lee Y, Kim J, Shin Y. Push-out bond strength evaluation of fiber-reinforced composite resin post cemented with self-adhesive resin cement using different adhesive bonding systems. Materials. 2021;14(13):3639. https://doi.org/10.3390/ma14133639.
25. Küden C, Karakaş SN. Photodynamic therapy and gaseous ozone versus conventional post space treatment methods on the push-out bond strength of fiber posts luting with different resin cements. Photodiagnosis Photodyn Ther. 2021;36:102586. https://doi.org/10.1016/j.pdpdt.2021.102586.
26. Santos FD, Banea M, Carlo H, De Barros S. Test methods for bond strength of glass fiber posts to dentin: A review. J Adhes. 2017;93(1–2):159–86. https://doi.org/10.1080/00218464.2016.1184094.
27. Goracci C, Tavares AU, Fabianelli A, Monticelli F, Raffaelli O, Cardoso PC, et al. The adhesion between fiber posts and root canal walls: comparison between microtensile and push-out bond strength measurements. Eur J Oral Sci. 2004;112(4):353–61. https://doi.org/10.1111/j.1600-0722.2004.00146.x.
28. Monticelli F, Toledano M, Tay FR, Cury AH, Goracci C, Ferrari M. Post-surface conditioning improves interfacial adhesion in post/core restorations. Dent Mater. 2006;22(7):602–9. https://doi.org/10.1016/j.dental.2005.05.018.
29. Ayad MF, Bahannan SA, Rosenstiel SF. Influence of irrigant, dowel type, and root-reinforcing material on fracture resistance of thin-walled endodontically treated teeth. J Prosthodont. 2011;20(3):180–9. https://doi.org/10.1111/j.1532-849X.2011.00687.x.
30. Galhano G, de Melo RM, Valandro LF, Bottino MA. Comparison of resin push-out strength to root dentin of bovine- and human-teeth. Indian J Dent Res. 2009;20(3):332–6. https://doi.org/10.4103/0970-9290.57378.
31. Yassen GH, Platt JA, Hara AT. Bovine teeth as substitute for human teeth in dental research: a review of literature. J Oral Sci. 2011;53(3):273–82. https://doi.org/10.2334/josnusd.53.273.
32. Chang Y-H, Wang H-W, Lin P-H, Lin C-L. Evaluation of early resin luting cement damage induced by voids around a circular fiber post in a root canal treated premolar by integrating micro-CT, finite element analysis and fatigue testing. Dent Mater. 2018;34(7):1082–8. https://doi.org/10.1016/j.dental.2018.04.006.
33. Gomes GM, Rezende EC, Gomes OM, Gomes JC, Loguercio AD, Reis A. Influence of the resin cement thickness on bond strength and gap formation of fiber posts bonded to root dentin. J Adhes Dent. 2014;16(1):71–8. https://doi.org/10.3290/j.jad.a30878.
34. Demiryürek EO, Külünk S, Yüksel G, Saraç D, Bulucu B. Effects of three Canal sealers on bond strength of a fiber post. J Endod. 2010;36(3):497–501. https://doi.org/10.1016/j.joen.2009.11.014.
35. Bakaus TE, Gruber YL, Reis A, Gomes OMM, Gomes GM. Bond strength values of fiberglass post to flared root canals reinforced with different materials. Braz Oral Res. 2018;32:e13. https://doi.org/10.1590/1807-3107bor-2018.vol32.0013.
36. Penelas AG, Piedade VM, Borges AC, Poskus LT, da Silva EM, Guimarães JG. Can cement film thickness influence bond strength and fracture resistance of

fiber reinforced composite posts? Clin Oral Investig. 2016;20(4):849–55. https://doi.org/10.1007/s00784-015-1568-3.
37. Peixoto RF, Aguiar CR, Jacob ES, Macedo AP, Mattos MGC, Antunes RPA. Influence of temporary cements on the bond strength of self-adhesive cement to the metal coronal substrate. Braz Dent J. 2015;26(6):637–41. https://doi.org/10.1590/0103-6440201300362.

Publisher's Note

Springer Nature remains neutral with regard to jurisdictional claims in published maps and institutional affiliations.